# Effects of freeze-thaw cycles on anisotropic deformation and microstructure of sand-bentonite mixtures

Farimah Arab*1, Hamed Sadeghi1, Mostafa Gholami1, and Pouya AliPanahi1

1*Department of Civil Engineering, Sharif University of Technology, Tehran, Iran*
**Corresponding author's email:* farimah.arab@sharif.edu

**Abstract:** The behavior of Bentonite-sand mixture under freeze-thaw (F-T) cycles plays an important role in the design of engineered buffer systems due to its sensitivity to temperature fluctuations. The hydro-mechanical properties of expansive soils are profoundly affected by these cycles in cold-region engineering. Therefore, the changes in dimensional parameters including anisotropic strain, and microstructural evolution of sand-bentonite mixtures are examined in this study to understand the complexities of soil responses to F-T cycles. To achieve this goal, a series of laboratory tests were conducted on cubic specimens subjected to F-T cycles (0 to 9 cycles), with varying bentonite contents (i.e., 70%, 40%, 10% by weight) and saturation levels (dry, optimum water content, and saturated) within two temperature-controlled chambers for freezing and thawing. Results indicated that volumetric strain increases with bentonite content, with specimens exhibiting significant shrinkage during freezing and expansion during thawing. The highest strain variation was observed in the B70-Opt specimen (6.38%), while the lowest value measured for the 10% bentonite mixture was nearly zero. Anisotropic behavior was noted, with predominant vertical strain in saturated specimens and horizontal strain dominance in dry and optimum conditions. Preliminary microstructural observations provided detailed insights into the observed microstructural changes.

## Introduction

Expansive soils are widely distributed worldwide and are characterized by high plasticity and sensitivity to moisture content variations [1; 2]. These soils are among the most problematic in engineering structures, as they can cause significant damage and pose major challenges in geotechnical engineering. The major problem associated with expansive soils is their tendency for volume change [3]. They undergo substantial swell-shrink deformation as water content changes, resulting in alterations in bulk volume, microstructure, and engineering properties such as shear strength, permeability, and volumetric behavior. In cold regions, expansive soils are not only affected by environmental factors like evaporation and rainfall, which alter their water content but also by freeze-thaw (F-T) cycles [4]. In seasonally frozen regions, soils typically experience at least one F-T cycle annually. These cycles can cause significant volumetric changes, leading to structural modifications, cracking, altered pore distribution, and notable impacts on mechanical and hydraulic properties [5].

Sand-bentonite mixtures, a type of expansive soil, are widely used in engineered applications such as landfill liners. They are valued for their favorable properties, including low hydraulic conductivity, cost-effectiveness, and resilience to environmental stresses. These mixtures act as barriers to isolate contaminants and minimize pollutant migration [6; 7]. However, their performance under F-T cycles remains a critical concern. Bentonite, a key component of sand-bentonite mixtures, is particularly affected by F-T cycles, which induce severe deformation, significantly altering its bulk volume and microstructure. Repeated freezing and thawing can cause the growth of macropores, microcracking, and irreversible structural changes, compromising their long-term effectiveness [8]. The initial F-T cycles are especially critical, as they significantly influence the soil's pore structure and aggregate stability [9]. Studies show that volume deformation during F-T cycles is closely related to factors such as initial water content, physical properties, and the number of F-T cycles. Saturated soils typically exhibit freeze-swelling, while soils with lower water content are prone to freeze-shrinkage [8]. Most studies on sand-bentonite mixtures and expansive soils under F-T cycles have focused on bulk volumetric changes. Limited attention has been given particularly to the separate horizontal and vertical deformation of soils [10; 11]. Understanding anisotropic dimensional changes is essential for investigating landform evolution, mitigating geological disasters, and constructing stable earth structures, especially in seasonally frozen regions.

This study aims to investigate the volumetric and anisotropic dimensional changes in sand-bentonite mixtures under varying saturation states and bentonite contents subjected to F-T cycles. Analyzing directional deformations, this research provides insights for the design of resilient geo-environmental structures, highlighting the importance of anisotropy in soil deformation and its implications for the stability and performance of engineered barriers in cold regions.

## Materials and Methods

### *Soil properties*

The soil used in this study comprised sand-bentonite mixtures, prepared by combining Firuzkuh sand with different proportions of commercial bentonite: 10%, 40%, and 70% bentonite content. Figure 1(a) illustrates the particle size distribution curves for the sand-bentonite mixtures with 10%, 40%, and 70% bentonite content. According to the Unified Soil Classification System (USCS), sand-bentonite mixtures with 10%, 40%, and 70% bentonite content are classified as silty clay of low plasticity (CL-ML), silt of high plasticity (MH), and clay of high plasticity (CH), respectively. Compaction tests were conducted using the standard effort method [12]. Figure 1(b) presents the compaction test results for the studied sand-bentonite mixtures and the initial conditions of the prepared specimens. Based on the compaction tests, the maximum dry unit weights for the soil specimens with 10%, 40%, and 70% bentonite content are 18.71 kN/m$^3$, 16.77 kN/m$^3$, and 14.8 kN/m$^3$, respectively. Additionally, the specific gravity of the soil mixtures was 2.70, 2.69, and 2.68 for the 10%, 40%, and 70% mixtures, respectively. Furthermore, the Atterberg limit test results indicate that the plastic limits of the soil mixtures are 18%, 30%, and 30%, while their corresponding plasticity indices are 5, 24, and 44, respectively.

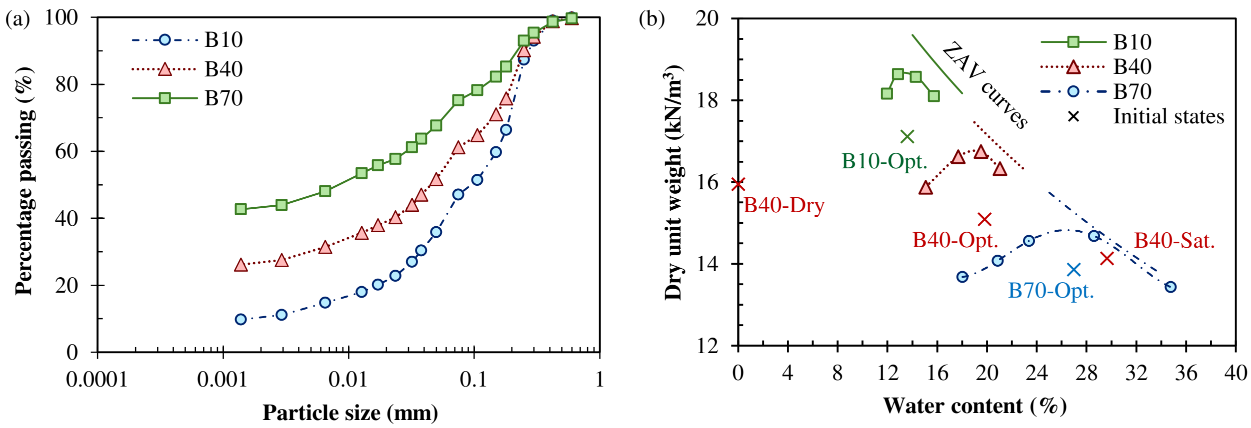


Figure 1: (a) Particle size distribution for Firuzkuh soil and commercial bentonite [12], and (b) compaction curves and initial conditions of specimens with varying bentonite content.

***Specimen preparation***

The commercial bentonite and Firuzkuh sand were first oven-dried. The dried materials were then mixed in three different ratios—1:9, 4:6, and 7:3 (bentonite to sand)—to prepare specimens labeled as B10, B40, and B70, respectively. A detachable four-part mold was used instead of conventional cylindrical molds to compact the sand-bentonite mixtures [13]. All specimens were compacted using a consistent procedure, and the applied compaction energy during specimen preparation was approximately 1234.22 Joules. After compaction, the specimens were extracted from the molds, weighed, and sealed with cling film to prevent moisture exchange with the environment, thus maintaining their initial water content. Figure 2 illustrates the specimens after compaction, sealing, and labeling. This procedure was followed for preparing specimens with optimum water content used in freeze-thaw cycle tests. For preparing dry and saturated specimens, additional steps were performed before sealing. It is important to note that all specimens were compacted at their corresponding optimum water contents and at 95% of their maximum dry density, according to compaction curves. For the dry specimen, the specimen was air-dried after extraction from the mold and then oven-dried to ensure complete moisture removal. Once dried, it was sealed and handled in the same manner as the other specimens. For the saturated specimen, the sample was saturated using a triaxial permeameter apparatus. For sample preparation, the cubic soil sample is encased in a rubber membrane and placed within a cell. The cell is filled with water, which applies confining pressure to the specimen, while de-aired water is circulated through the sample from bottom to top to achieve uniform saturation throughout the specimen. After saturation, the specimen was extracted from the triaxial apparatus, sealed, and processed consistently with the other specimens.

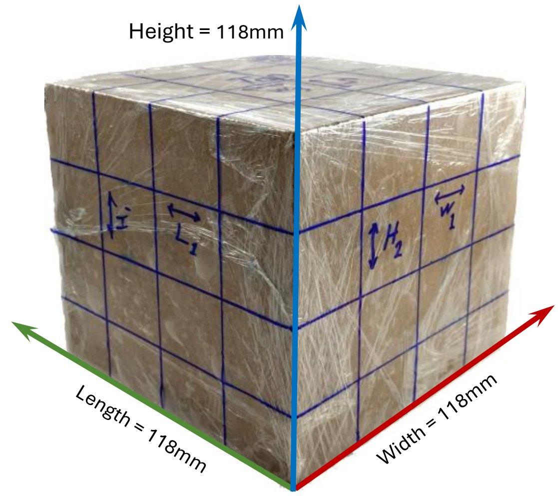


Figure 2: A typical cubic test specimen wrapped in cling film with labeled dimensions.

***Freezing-thawing tests***

Freeze-thaw cycles were applied to the specimens using two temperature-controlled chambers. All freeze-thaw tests were conducted in a closed three-dimensional system. Figure 3(a) shows the freezer, and Figure 3(b) shows the incubator used during the freeze-thaw cycles. The sealed and labeled specimens were initially placed in the freezing chamber for 48 hours, followed by transfer to the thawing chamber for another 48 hours. Consequently, each freeze-thaw cycle lasted 96 hours. The freeze-thaw temperature range was selected based on temperature data from Damavand and Firuzkuh cities, provided by the Iran Meteorological Organization for the years 2012 to 2022. Firuzkuh was chosen as the origin of the sand used in the sand-bentonite mixture. Damavand, being nearby, was included to provide additional regional context. These two neighboring cities in Tehran Province were considered representative of the highly populated region, and a temperature range of -15°C to +15°C was selected to simulate realistic freeze-thaw conditions.

Five specimens were chosen for the freeze-thaw tests: three were in unsaturated conditions, with sand-bentonite mixtures at their respective optimum water contents. These specimens were labeled B10-Opt., B40-Opt., and B70-Opt., referring to samples with 10%, 40%, and 70% bentonite content at optimum saturation levels. Additionally, one dry specimen and one saturated specimen were tested, labeled as B40-Dry and B40-Sat., respectively, both containing 40% bentonite by weight. Each specimen underwent nine freeze-thaw cycles except for B70-Opt., which could not complete the cycles due to significant crack formation that made volume measurements unreliable. Accordingly, the volume and dimensional changes of the specimens were measured after each freeze-thaw stage. For each specimen, the height (H), length (L), and width (W) were recorded. As shown in Figure 2, dimensions were labeled for cubic samples, resulting in six measurement lines on each cube face. To enhance measurement accuracy, each line was measured during every session, and the average value for each dimension was taken as the final value. Measurements were performed using an electronic vernier caliper with a precision of 0.01 mm. Finally, a Field Emission Scanning Electron Microscopy (FESEM) test was conducted on an intact B40-Opt specimen and a B40-Opt specimen that underwent freeze-thaw cycles. The FESEM analysis was performed to examine changes in the microstructure and compare the specimen's microstructure before and after the freeze-thaw cycles.

(a) Freezer (b) Incubator

Figure 3: Experimental setup showing (a) a freezer, and (b) an incubator used for freeze-thaw cycles.

**Results and discussion**

The volumetric strain of B10-Opt, B40-Opt, and B70-Opt during the freezing and thawing stages is illustrated in Figure 4. As shown, the initial stage of each specimen is represented at x = 0, the first freezing stage at x = 0.5, and the first thawing stage at x = 1. Subsequent cycles follow the same pattern. In this figure, the suffix "-F" in sample labels (e.g., B10-Opt-F) indicates the volumetric strain measured during the freezing stage of the corresponding cycle, while the suffix "-T" (e.g., B10-Opt-T) represents the strain during the thawing stage. According to Figure 4, a positive volumetric strain value indicates expansion, while a negative value represents shrinkage. Figure 4(a) shows that the specimen with 10% bentonite (B10-Opt) exhibits negligible volumetric strain due to freeze-thaw cycles. Conversely, as presented in Figure 4(b) and 4(c), high bentonite content specimens shrink during the freezing stages and expand during the thawing stages. The strain range in B40-Opt is greater than in B10-Opt, but the enclosed area between the freezing and thawing curves remains almost unchanged. As shown in Figure 4(c), the B70-Opt specimen exhibits higher volumetric strains compared to B40-Opt and B10-Opt, particularly during the freezing stages of the freeze-thaw cycles. The enclosed area between the freezing and thawing curves is the largest among the three specimens.

Moreover, the strain induced during the thawing stages increases with successive freeze-thaw cycles. It is worth noting that the negligible volumetric strain observed in the B10-Opt specimen, compared to the B40-Opt and B70-Opt mixtures, is attributed to its lower bentonite content and plasticity. In this mixture, bentonite does not significantly influence the soil structure, and the volumetric response is primarily governed by the sand fraction, which is less sensitive to freeze-thaw-induced deformation.

In comparison, the strain range for B40-Opt is from -1.73% to 1.07%, while for B70-Opt, it is from -4.72% to 1.66%, indicating a larger range for B70-Opt. Additionally, the final volumetric strains of the specimens after completing all freeze-thaw cycles are 0.12%, 1.02%, and 1.55% for B10-Opt, B40-Opt, and B70-Opt, respectively, with B70-Opt having the highest value. The higher strain observed under freeze-thaw cycles in specimens with higher bentonite content is attributed to the significant role of bentonite as a structural controller within the soil matrix. In simpler terms, the greater the bentonite content in the soil, the higher the potential for volumetric changes, as observed in the B70-Opt specimen [14]. Conversely, in specimens with a higher sand content, the addition of sand reduces the volumetric variation of the material. This implies that bentonite no longer dominates the control of the soil matrix; instead, the structure and volumetric behavior become dependent on sand.

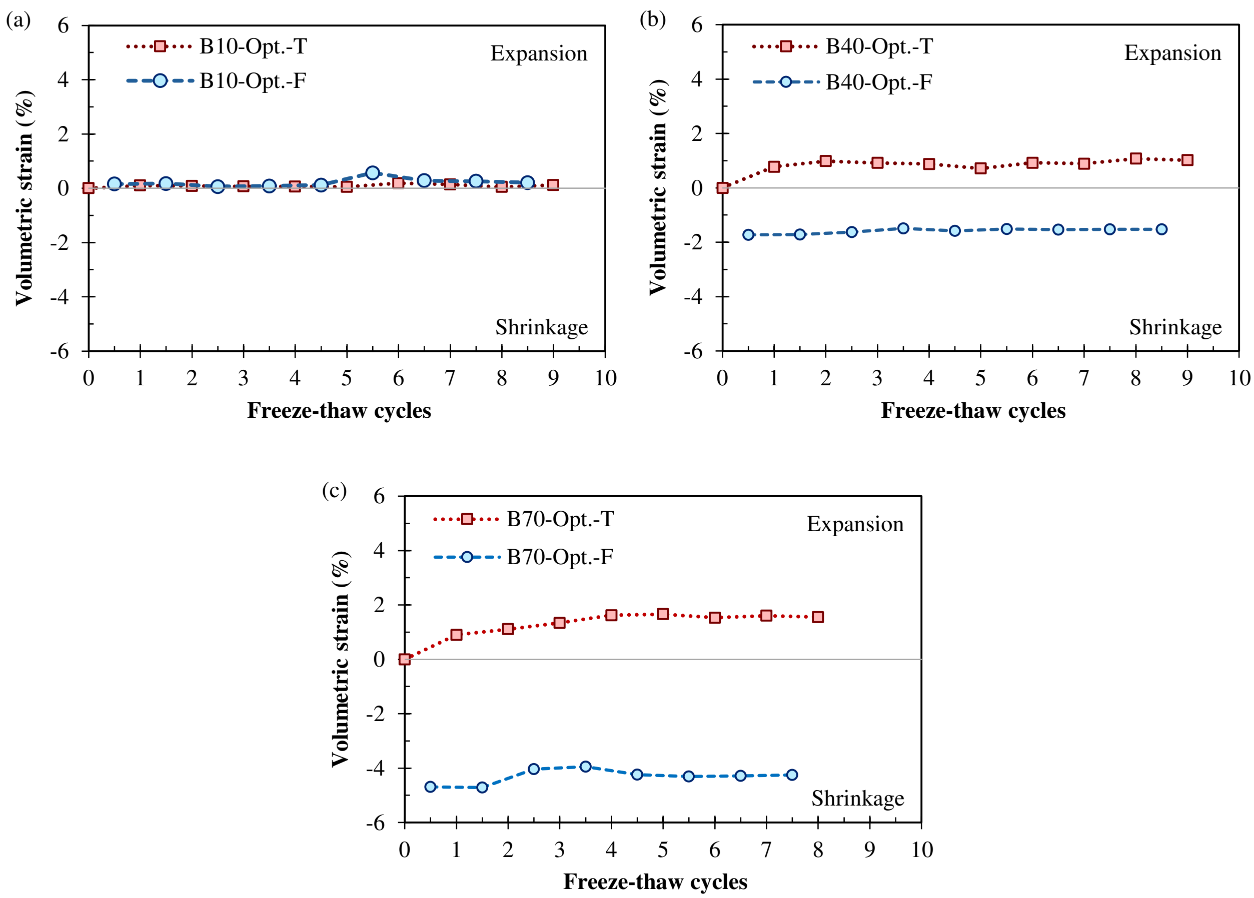


Figure 4: Variation of volumetric strain as a function of freeze-thaw cycles for different bentonite contents: (a) B10-Opt., (b) B40-Opt., and (c) B70-Opt.

In both B40-Opt and B70-Opt specimens, freezing-induced shrinkage was observed due to cryogenic suction and ice lens formation [15]. This suction occurs because of the unsaturated state and low water content of the specimens. During freezing, a thermal gradient forms within the specimen, with the surface temperature being lower than the interior. These gradient drives intra-aggregate water outward into inter-aggregate pore spaces, causing desiccation-induced contraction. Additionally, Ice lens formation in inter-aggregate pores generates surface pressure, which leads to rearrangement of soil particles. While ice formation increases the size of inter-aggregate pores, this expansion is less significant in specimens compared to the shrinkage caused by suction and particle rearrangement, resulting in overall volumetric contraction during freezing. Upon thawing, water returns to intra-aggregate pore spaces. This is due to the temperature gradient between the warmer surface and the colder interior. Additionally, the expansion of inter-pore spaces caused by ice formation contributes to non-reversible soil volume change. This results in volumetric expansion after thawing.

The first time a dimensionless geometry factor was proposed, anisotropy in the volume change behavior of soils can be described using the theory of the geometry factor [16]. In this study, the geometry factor is defined as the relationship between horizontal and vertical strain [17]. It is calculated as shown in Eq. (1):

$$r_s = \frac{\ln V_n/V_0}{\ln z_n/z_0} \tag{1}$$

where $V_0$ and $V_n$ represent the volume of the soil in its initial condition and at the n$^{th}$ cycle, respectively, and $z_n$ and $z_0$ represent the height of the specimen at the n$^{th}$ cycle and in the initial condition, respectively. A shrinkage ratio of 1 reflects only vertical deformation in the specimen. Moreover, a shrinkage ratio between 1 and 3 indicates that vertical deformation is dominant. Meanwhile, a ratio of exactly 3 represents isotropic deformation, while ratios above 3 suggest predominant horizontal deformation.

In this study, the definition of shrinkage ratio ($r_s$) is utilized for studying the anisotropic deformation of B40 specimens at three different saturation levels (dry, optimum, and saturated) under freeze-thaw cycles, as shown in Figure 5. Specifically, Figure 5(a) presents the $r_s$ during the freezing stages, while Figure 5(b) displays the $r_s$ during the thawing stages. As presented in Figure 5(a), during the freezing stages, the B40-sat specimen exhibits predominant vertical strain behavior. Interestingly, the predominance of vertical strain remains consistent as the number of freezing stages increases. In contrast, the B40-dry and B40-opt specimens have $r_s$ values greater than 3, signifying that horizontal strain is predominant in these specimens. Notably, the horizontal strain dominance does not change with repeated freezing stages for these two specimens. It is important to highlight that in the B40-opt specimen, the $r_s$ value shows an increasing trend with the number of freeze-thaw cycles. This trend occurs because the vertical strain of the specimen progressively decreases with an increasing number of freeze-thaw cycles. However, the horizontal strain remains the predominant contributor to volumetric changes in the B40-Opt specimen.

As shown in Figure 5(b), during the thawing stages, the strain behavior of the specimens remains unchanged with an increasing number of cycles. Notably, the strain behavior of B40-sat and B40-dry remains consistent between the freezing and thawing stages. However, B40-Opt exhibits predominant vertical strain behavior during the thawing stages, in contrast to the horizontal strain dominance observed during the freezing stages. This indicates that while the number of freeze-thaw cycles does not affect the strain behavior of B40-Opt, the state of the specimen—whether frozen or thawed—plays a significant role in determining its strain behavior.

The consistent strain behavior of B40-dry in both the freezing and thawing stages is likely due to its minimal volumetric strain during freeze-thaw cycles. The predominant horizontal strain observed in this specimen can be attributed to the effects of its drying process. In the frozen state, the B40-Opt exhibited the least shrinkage in height compared to the other dimensions. As the number of freeze-thaw cycles increased, the vertical strain approached zero, while the horizontal strain remained more pronounced during freezing (Figure 5(a)). Conversely, during thawing, the specimen showed the greatest expansion in height, with the other dimensions contributing less to the overall volume increase, as shown in Figure 5(b). For the B40-Sat, an increase in volume was observed during freezing, with the height experiencing the largest strain. Upon thawing, plastic deformation caused positive strain in all dimensions, but the height continued to show greater strain than the horizontal direction. This behavior led to the specimen exhibiting predominantly vertical strain in both frozen and thawed states. This vertical strain shift in the B40-opt and B40-sat samples is attributed to the specimen preparation process and the particle arrangement. The particles predominantly aligned horizontally due to vertical compaction. Accordingly, the specimen tends to be more compressible in the horizontal direction than in the vertical direction. This results in more significant shrinkage-induced compressive strain in the radial direction, indicating that the sample has a cross-anisotropic nature.

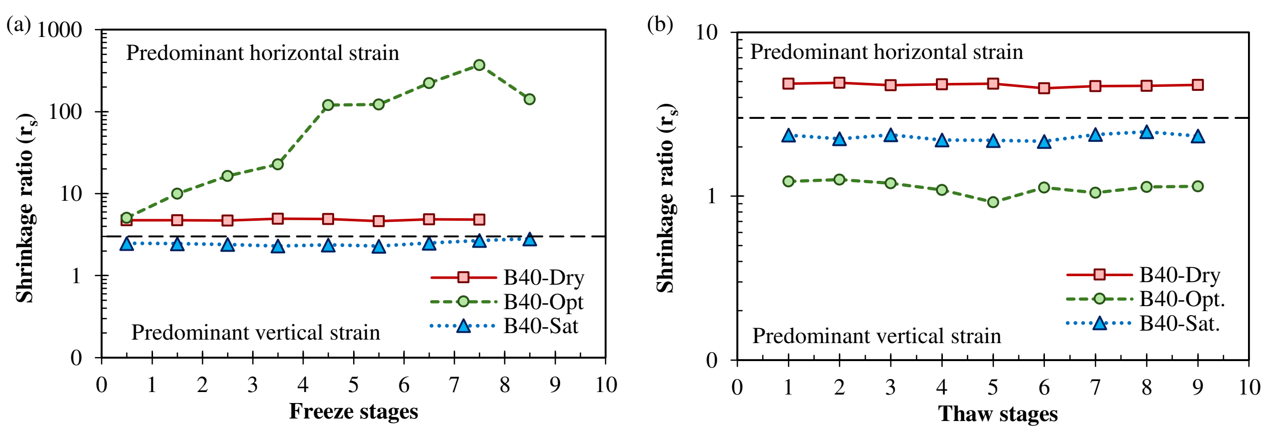


Figure 5: Variation in shrinkage ratio as a function of (a) freeze stages, and (b) thaw stages at different saturation levels for B40 specimens.

Figure 6 presents the FESEM images of the B40-Opt specimen before and after undergoing freeze-thaw cycles. As illustrated in the images, notable microstructural changes are observed in the specimen due to these cycles. Specifically, the freeze-thaw cycles have resulted in the enlargement of existing pores and the formation of cracks within the structure of the specimen. These microstructural alterations align with the observed volumetric changes, particularly the plastic deformation and increase in overall specimen volume after repeated freeze-thaw cycles.

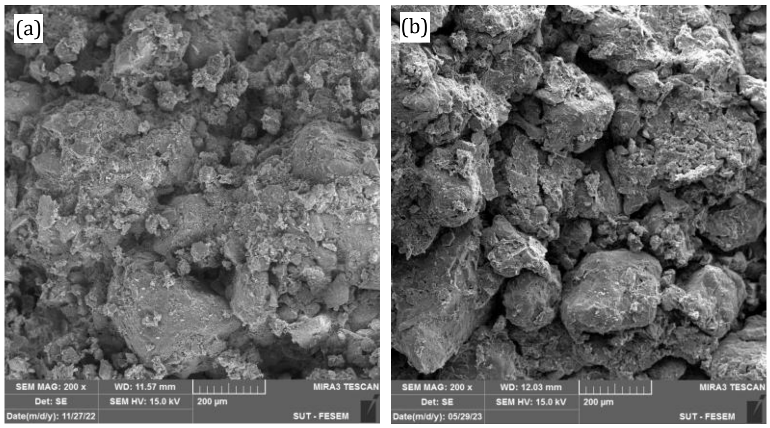


Figure 6: FESEM images of soil microstructure: (a) before and (b) after three freeze-thaw cycles.

**Conclusions**

To investigate the effects of freeze-thaw (F-T) cycles on the volumetric strain and anisotropic deformation of sand-bentonite mixtures with varying bentonite contents and in different saturation levels series of laboratory tests have been conducted. The results from the tests conducted on B10-Opt, B40-Dry, B40-Opt, B40-Sat, and B70-Opt specimens offer several key insights:

The volumetric strain behavior of specimens under F-T cycles was significantly influenced by the bentonite content. The B10-Opt specimen, with low bentonite content, exhibited negligible volumetric strain, indicating that minimal changes occurred during freezing and thawing. In contrast, the specimens with higher bentonite content, B40-Opt, and B70-Opt, experienced notable shrinkage during freezing and expansion during thawing, with the range of strain increasing as the bentonite content increased. Specifically, B70-Opt showed the largest strain variation, reaching -4.72% during freezing and 1.66% during thawing. These results emphasize the important role of bentonite as a structural controller, which significantly influences the volumetric behavior of the soil matrix.

During the freezing stages, the B40-sat specimen experiences predominant vertical strain, while the B40-dry and B40-opt specimens show horizontal strain dominance. Additionally, B40-opt exhibits an increasing trend in shrinkage ratio ($r_s$) with the number of cycles, indicating a decrease in vertical strain over time. During thawing, strain behavior remains consistent for B40-sat and B40-dry, whereas B40-opt shifts to predominant vertical strain, suggesting that specimen state plays a key role in strain behavior. These findings highlight the anisotropic and cross-anisotropic nature of the specimens, influenced by the particle arrangement and preparation process.

In conclusion, the findings of this study underline the significant role of bentonite content in shaping the freeze-thaw behavior of soil mixtures. The volumetric strain behavior is highly influenced by the bentonite content, with higher bentonite percentages leading to more substantial volumetric changes. These insights can guide the design and performance predictions for materials used in cold regions, where freeze-thaw cycles play a crucial role in soil behavior.

**References**


[1] H. Sadeghi and P. AliPanahi. Saturated hydraulic conductivity of problematic soils measured by a newly developed low-compliance triaxial permeameter. Engineering Geology, 278:105827, 2020.

[2] H. Sadeghi, A. Hasani Motlagh, A. Golaghaei Darzi, P. AliPanahi, S. Khodadadi, and D. Song. Measurement and modeling of the saturated hydraulic conductivity functions of collapsible and expansive soils. International Journal of Geomechanics, 24(4):04024039, 2024.

[3] L. Niu, A. Zhang, J. Zhao, W. Ren, Y. Wang, and Z. Liang. Study on soil-water characteristics of expansive soil under the dry-wet cycle and freeze-thaw cycle considering volumetric strain. Advances in Civil Engineering, 2021(1):6622370, 2021.

[4] G. T. Zhao, Z. Han, W. L. Zou, and X. Q. Wang. Evolution of mechanical behaviours of an expansive soil during drying-wetting, freeze–thaw, and drying-wetting-freeze–thaw cycles. Bulletin of Engineering Geology and the Environment, 80(10):8109–8121, 2021.

[5] Q. Chen, B. Ghimire, L. Su, and Y. Liu. Micro-scale investigations on the mechanical properties of expansive soil subjected to freeze-thaw cycles. Cold Regions Science and Technology, 219:104128, 2024.

[6] A. Hedayati-Azar, H. Sadeghi, A. G. Darzi, and P. AliPanahi. Numerical modelling of soluble contamination transport in landfills based on empirical function of membrane efficiency. In International Conference on Environmental Geotechnology, Recycled Waste Materials and Sustainable Engineering, pp. 183–198. Singapore: Springer Nature Singapore, 2022.

[7] M. Gholami, H. Sadeghi, and P. Alipanahi. Anisotropic hydraulic conductivity of as-compacted, bare and vegetated soils. Géotechnique, 1–14, 2024.

[8] H. Wang, X. Li, W. Xin, V. N. Paramonov, and X. Zhao. Influence of relative compaction and degree of saturation on the deformation characteristics of bentonite under freeze-thaw cycles. Research in Cold and Arid Regions, 15(4):161–170, 2023.

[9] J. Li, H. Chen, X. Gao, Q. Ding, W. Shan, H. Guo, and J. Zhuo. Cracks evolution and micro mechanism of compacted clay under wet-dry cycles and wet-dry-freeze-thaw cycles. Cold Regions Science and Technology, 214:103944, 2023.

[10] P. Alipanahi, M. Gholami, H. Sadeghi, and A. H. Motlagh. Development of a cube triaxial permeameter for evaluation of anisotropic permeability of vegetated soils.

[11] Y. Zhang, Y. Lu, S. Liu, B. Fang, Z. Li, and K. Liu. Volumetric behavior of an unsaturated clayey soil-rock mixture subjected to freeze-thaw cycles: A new insight. Cold Regions Science and Technology, 201:103608, 2022.

[12] ASTM D698-12. Standard Test Methods for Laboratory Compaction Characteristics of Soil Using Standard Effort (12,400 ft-lbf/ft3 (600 kN-M/m3)). ASTM International, West Conshohocken, PA, USA, 2012.

[13] H. Sadeghi, M. Gholami, P. AliPanahi, and D. Song. The influence of isotropic loading and unloading on anisotropic evolution of saturated hydraulic conductivity of bentonite-sand mixtures in a cube triaxial permeameter. Engineering Geology, 331:107454, 2024.

[14] M. Y. Fattah, N. M. Salim, and E. J. Irshayyid. Determination of the soil–water characteristic curve of unsaturated bentonite–sand mixtures. Environmental Earth Sciences, 76(5):201, 2017.

[15] F. Arabchobdar, H. Sadeghi, M. Gholami, and P. AliPanahi. Multi-directional deformation and hydraulic conductivity of expansive soils subjected to freeze-thaw cycles from three distinct initial saturation levels. Journal of Rock Mechanics and Geotechnical Engineering, 2024.

[16] J. J. B. Bronswijk. Shrinkage geometry of a heavy clay soil at various stresses. Soil Science Society of America Journal, 54(5):1500–1502, 1990.

[17] S. Gebhardt, H. Fleige, and R. Horn. Anisotropic shrinkage of mineral and organic soils and its impact on soil hydraulic properties. Soil and Tillage Research, 125:96–104, 2012.

# INTERNATIONAL SOCIETY FOR SOIL MECHANICS AND GEOTECHNICAL ENGINEERING

*This paper was downloaded from the Online Library of the International Society for Soil Mechanics and Geotechnical Engineering (ISSMGE). The library is available here:*

*https://www.issmge.org/publications/online-library*

*This is an open-access database that archives thousands of papers published under the Auspices of the ISSMGE and maintained by the Innovation and Development Committee of ISSMGE.*

*The paper was published in the proceedings of the 4th Pan-American Conference on Unsaturated Soils (PanAm UNSAT 2025) and was edited by Mehdi Pouragha, Sai Vanapalli and Paul Simms. The conference was held from June 22nd to June 25th 2025 in Ottawa, Canada.*